doi:10.20944/preprints201804.0337.v1

Type of the Paper (Article)

Application of a Hybrid Method for Power System Frequency Estimation with a 0.2-second Sampled Period

Chih-Hung Lee [1],* and Men-Shen Tsai [2, 3]

[1] Graduate Institute of Mechanical and Electrical Engineering, National Taipei University of Technology, Taipei, Taiwan; t100669021@ntut.edu.tw
[2] Graduate Institute of Automation Technology, National Taipei University of Technology, Taipei, Taiwan; mstsai@mail.ntut.edu.tw
[3] Research Center of Energy Conservation for New Generation of Residential, Commercial, and Industrial Sectors;
* Correspondence: t100669021@ntut.edu.tw; Tel.: +886-2-2771-2171(ext. 4374)

Featured Application: Authors are encouraged to provide a concise description of the specific application or a potential application of the work. This section is not mandatory.

Abstract: The signal processing technique is one of the principal tools for diagnosing power quality (PQ) issues in electrical power systems. The Discrete Fourier Transform (DFT) is a frequency analysis technique used to process power system signals and identify PQ problems. However, the DFT algorithm may lead to spectral leakage and picket-fence effect problems for asynchronously sampled signals that contain harmonic, inter-harmonic, and flicker components. To resolve this shortcoming, a hybrid method for frequency estimation based on a second-level DFT approach and a frequency-domain interpolation algorithm to obtain the accurate fundamental frequency of a power system is proposed in this paper. This method uses a second-level DFT to compute the cosine and sine parts for the fundamental frequency components of the acquired signals. Then, a frequency-domain interpolation approach is adopted to determine the amplitude ratio for the cosine and sine parts of the system's fundamental frequency. To demonstrate the performance of the proposed frequency estimation method, the observation window used by this paper to evaluate different estimation algorithms is 200 ms. According to the IEC standards, a 200 ms acquisition window is recommended for power system quality assessment. A set of mixed signals with harmonic, inter-harmonic, and flicker components with the fundamental frequency deviation is used. The evaluation results demonstrate the superiority of the new method over other approaches for assessing asynchronously sampled signals contaminated with noise, harmonic, inter-harmonic, and flicker components.

Keywords: frequency estimation, asynchronously sampled, harmonic, flicker.

1. Introduction

Power system signal analysis is a key step in PQ diagnosis. Effective extraction of power system signal features is helpful to understand the underlying physical nature of PQ's phenomena, and to evaluate its health condition, thereby providing convincing evidences for diagnosis. However, in both academic researches and engineering practices, power system signals are usually highly intricate. The vast increase usage in electronic devices may cause PQ problems such as harmonics, inter-harmonics, and voltage flickers in power systems. Such PQ problems may lead to power system, factory equipment, and public facility deviations or may even result in electrical equipment damage in severe cases.

The power system frequency is nonstationary. The degree of frequency change depends on the balance between power generation and load demand. Thus, the frequency is a key indicator for the safety and economy of the power system operation. A frequency below the nominal value represents an overloaded system; while a frequency above the nominal value represents a power oversupply. In general, the power system frequency is a critical indicator for power system monitoring, control, and protection [1-5]. Therefore, power system signal analysis is a key research topic and plays an important role in PQ diagnosis. International standards such as IEC-61000 have described the diagnosis of PQ.

In the past, several researches have successfully shown that the frequency assessment technology was able to detect the PQs of defects in power system. These technologies include Zero-crossing Algorithm [5-7], Discrete Fourier Transform (DFT) [8-13], Kalman Filter (KF) [14, 15], Phase-Locked Loops (PLL) [16, 17], Newton Algorithm [18, 19], Least squares Algorithm (LMS) [20, 21], Prony Algorithm [4, 22], Taylor Algorithm [23, 24], and Artificial-intelligence Algorithm [25, 26].

Among them, one of the two most popular techniques adopted is the Zero-crossing Algorithm, which has the least computational complexity and the fastest execution speed. However, this method is susceptible to noise and spikes, and can only provide an accurate frequency evaluation in noise-free and disturbance-free environments [5-7].

In [5], using the waveform construction method to combine the Time Domain Frequency Estimation Algorithm with the Newton Interpolation method was proposed. This approach can eliminate the leakage effect caused by the FFT (Fast Fourier Transform) calculation under asynchronous sampling conditions. In this paper, a Time Domain Zero-crossing Algorithm to evaluate the basic frequency is proposed. This algorithm uses the zero-crossing frequency detection method to calculate the basic frequency. Because this algorithm can be affected by non-basic frequency signals, a pre-filter must be used to eliminate the non-basic frequency signals. After the basic frequency has been obtained, Newton Interpolation method is applied to generate a new sample waveform that conforms to the FFT application conditions. As a result, the accurate basic frequency under asynchronous sampling conditions can be obtained.

In [6, 7], the authors proposed the digital filter and zero-crossing technique combination frequency evaluation method. They broke down the original sample signals into two orthogonal component waveforms using cosine and sine filters. These two waveforms and the zero-crossing technique are used to assess the basic frequency of the power system. The results indicated that the orthogonal filter and the zero-crossing technique can effectively reduce the noise and disturbance interferences.

The other technique that is popular used in calculating the fundamental frequency of a power system is DFT/FFT. In the IEC61000-4-30 standard, PQ measurement analysis is mostly based on DFT/FFT techniques. DFT/FFT can convert the periodic signals obtained via synchronous sampling into frequency domain data to help us learn more about the spectrum composition. However, the basic frequency of an actual power system will vary from time to time and become affected by noise, flickers, harmonic waves, inter-harmonic waves, and other disturbances. Therefore, it is unrealistic and impossible to achieve strict synchronous sampling without a special technique such as PLL (Phase Lock Loop). Asynchronous sampling would cause the DFT/FFT algorithm to create the spectral leakage and picket-fence effect problems and directly cause the FFT algorithm spectrum calculation accuracy to drop dramatically [8–13].

In [8], it was proposed to use the window method with DFT for frequency calculation, and to obtain the basic frequency parameter values according to the multi-point spectrum near the base frequency peak point as well as the Hanning window interpolation expressed as a function of the frequency domain itself. The results indicated that this multi-point frequency domain interpolation algorithm can effectively reduce the noise and disturbances.

Reference [9] adopted the pseudo-synchronization technique, Hanning window, and FFT combination for frequency calculation in order to improve the frequency estimation accuracy under the noise and disturbance effects. The author combined the original sample signals with the Hanning window function, performed FFT conversion for the new wave signals, and then assessed the basic frequency of the power system. The results indicated that the pseudo-synchronization technique combined with FFT can effectively reduce the noise and disturbances.

The PQ event detection algorithms require precise power system frequency which can be obtain using DFT-based frequency estimation algorithms under asynchronously-sampled signals that are contaminated with noise, flicker, and harmonic and inter-harmonic components. In this paper, we proposed a two-level DFT and frequency domain interpolation hybrid method to accurately calculate the basic frequency of a power system. This paper is divided into four chapters. Chapter 1 is the preface. Chapter 2 explores the two-level DFT and frequency domain interpolation hybrid method. Chapter 3 provides validation for the method. Chapter 4 concludes this paper.

2. Two-Level DFT and Frequency Domain Interpolation Hybrid Method

Frequency evaluation technology is the foundation of PQ analysis and monitoring. Therefore, excellent frequency assessment techniques can improve power system protection and monitoring. At present, the IEC61000-4-30 standard established by the International Electrotechnical Commission (IEC) for power quality-related measurement techniques is based on the DFT/FFT technique to analyze the PQ issues. To conform to

Preprints (www.preprints.org) | NOT PEER-REVIEWED | Posted: 26 April 2018 doi:10.20944/preprints201804.0337.v1

the standard and facilitate development, numerous monitoring devices have adopted the fixed sampling frequency-based DFT technique in order to simplify device design. However, the basic electricity frequency changes may lead to asynchronous sampling problems for fixed sampling frequency devices, which may cause leakage effects during the DFT calculations. In addition, if the sampling frequency and calculation method window are not divisible, it would also cause the DFT method to obtain inaccurate basic frequencies.

The primary implementation steps of this paper are shown in Figure 1. First, we calculated the DFT orthogonal coefficient and amplitude ratio deviation coefficient based on the power signals captured. Next, we created two levels of orthogonal filtering based on the DFT orthogonal coefficients and power signals calculated. We then used the two orthogonal filtering signals and frequency domain interpolation to determine the amplitude ratio needed for the frequency calculation. Finally, we used the amplitude ratio and the amplitude ratio deviation coefficient to calculate the frequency more precisely.

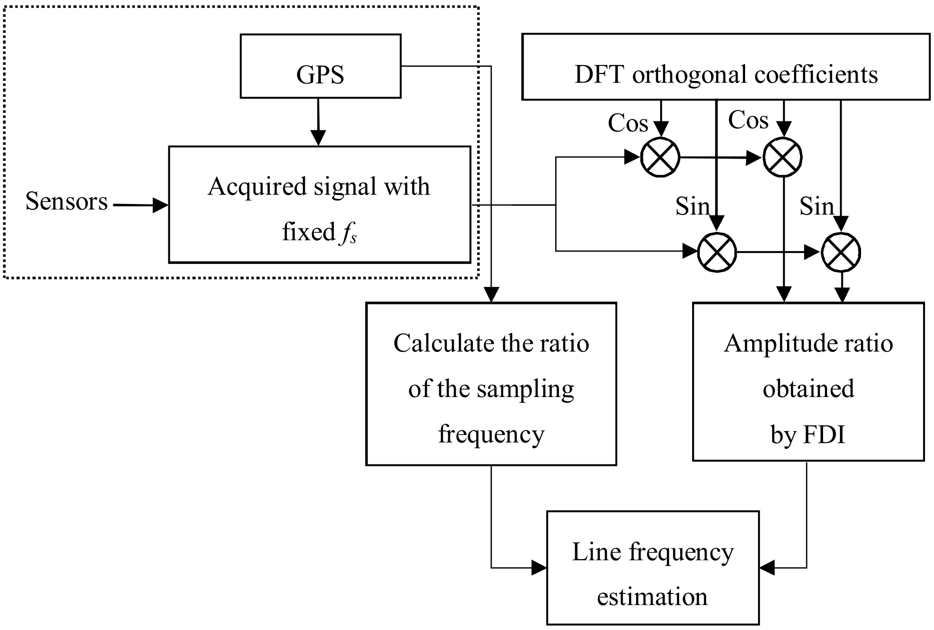

Figure 1. Proposed frequency assessment process.

2.1. DFT Orthogonal Filter Coefficients

The actual power system signals (such as voltage and current) can be expressed in discrete time with three parameters: amplitude (A), frequency (f), and phase (θ), as shown in Equation (1).

$$x(n) = A \cdot \cos\left(2\pi \frac{f_a \cdot n}{f_s}\right), n = 0,1,\ldots N-1$$
$$f_s = f_0 \cdot N_0 \tag{1}$$

In (1), f_s is the sampling frequency, f_0 is the nominal frequency, f_a is the actual frequency, N_0 is the number of samples per cycle, and N is the total number of samples.

We used the DFT to convert the sample's N-point discrete signals into the N-point spectrum energy. The DFT formula is shown in Equation (2).

$$X(i) = \frac{2}{N}[\sum_{n=0}^{N-1} x(n)\cos(2\pi \frac{f_a}{f_0 \cdot N_0} n) - j\sum_{n=0}^{N-1} x(n)\sin(2\pi \frac{f_a}{f_0 \cdot N_0} n)] \tag{2}$$

Assuming there is a single window with M-point samples, Equation (2) can be expanded as follows:

$$\begin{aligned}\mathrm{X}(i) = &\frac{2}{M}\left(x(1)\cos(2\pi\frac{f_a}{f_0\cdot N_0}) + x(2)\cos(4\pi\frac{f_a}{f_0\cdot N_0}) + \ldots + x(M)\cos(2\pi\frac{f_a}{f_0}) \right) \\ &+ j\frac{2}{M}\left(x(1)\sin(2\pi\frac{f_a}{f_0\cdot N_0}) + x(2)\sin(4\pi\frac{f_a}{f_0\cdot N_0}) + \ldots + x(M)\sin(2\pi\frac{f_a}{f_0}) \right)\end{aligned} \tag{3}$$

Therefore, for the i-th data window, the sine and cosine components can be expressed as Equations (4) and (5).

$$A(i) = \frac{2}{M}\sum_{\mathrm{n}=i}^{M+i-1} x(i)\cos(2\pi\frac{f_a}{f_0\cdot N_0}n) \tag{4}$$

$$B(i) = \frac{2}{M}\sum_{\mathrm{n}=i}^{M+i-1} x(i)\sin(2\pi\frac{f_a}{f_0\cdot N_0}n) \tag{5}$$

If the fundamental signal frequency is equal to the assumed basic frequency (f_a=f_0), then Equations (4) and (5) are orthogonal to each other. At this point, A(t) and B(t) represent pure cosine and pure sine wave forms, respectively. In Figure 2, the orthogonal filter has different amplitude responses for all frequencies other than the nominal frequency. Its different amplitude response results clearly indicated that, when the orthogonal filter conforms to f_a=f_0 (60 Hz), the amplitude response value is 1.

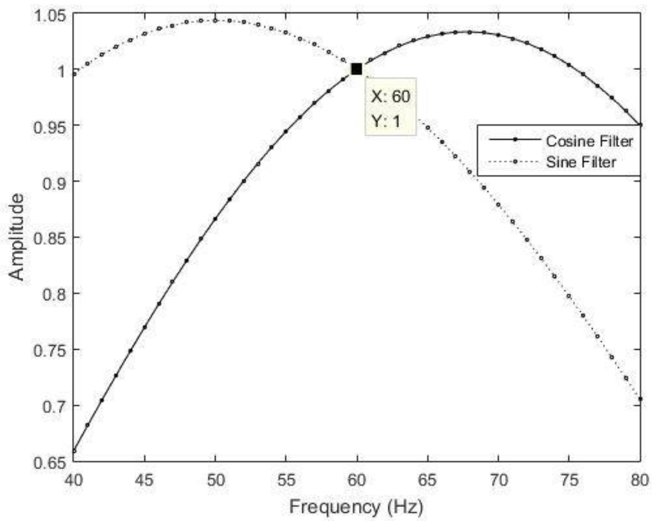

Figure 2. Frequency impact of the orthogonal filter.

2.2. Frequency Estimation Algorithm

In summary, we can derive the frequency change rules based on the amplitude response characteristics described above, and thus calculate the exact frequency. In practical applications, the usable vector lengths for the cosine and sine coefficients of the two orthogonal filters have the vector matrix of N_0 as expressed by Equations (6) and (7).

$$CosWindow = \frac{2}{N_0}\left[\left(\cos(\frac{2\pi}{N_0}+\frac{\pi}{N_0}), \cos(\frac{4\pi}{N_0}+\frac{\pi}{N_0}), \ldots + \cos(2\pi\frac{N_0-1}{N_0}+\frac{\pi}{N_0}) + \cos(2\pi+\frac{\pi}{N_0}) \right)\right] \tag{6}$$

$$SinWindow = \frac{2}{N_0}\left[\left(\sin(\frac{2\pi}{N_0}+\frac{\pi}{N_0}), \sin(\frac{4\pi}{N_0}+\frac{\pi}{N_0}), \ldots + \sin(2\pi\frac{N_0-1}{N_0}+\frac{\pi}{N_0}) + \sin(2\pi+\frac{\pi}{N_0}) \right)\right] \tag{7}$$

Performing unilateral Z conversion for Equations (6) and (7), their amplitude response functions can be expressed as Equations (8) and (9) [10].

$$\left|H_{CosWindow}(f)\right| = \frac{4}{N_0} \cdot \frac{\cos\left(\frac{\pi}{N_0}\right)\sin\left(\frac{\pi}{N_0}\frac{f}{f_0}\right)\sin\left(\pi\frac{f}{f_0}\right)}{\cos\left(\frac{2\pi}{N_0}\frac{f}{f_0}\right) - \cos\left(\frac{2\pi}{N_0}\right)} \tag{8}$$

$$\left|H_{SinWindow}(f)\right| = \frac{4}{N_0} \cdot \frac{\sin\left(\frac{\pi}{N_0}\right)\cos\left(\frac{\pi}{N_0}\frac{f}{f_0}\right)\sin\left(\pi\frac{f}{f_0}\right)}{\cos\left(\frac{2\pi}{N_0}\frac{f}{f_0}\right) - \cos\left(\frac{2\pi}{N_0}\right)} \tag{9}$$

Equations (8) and (9) can be used to derive the amplitude ratio of the two filters, and this ratio can be expressed as Equation (10).

$$R_{atio} = \frac{A}{B} = \frac{\left|H_{CosWindow}(f)\right|}{\left|H_{SinWindow}(f)\right|} = \frac{\tan\left(\frac{\pi}{N_0}\frac{f}{f_0}\right)}{\tan\left(\frac{\pi}{N_0}\right)} \tag{10}$$

Finally, the basic power signal frequency can be deduced using the amplitude value obtained using Equation (10), and the basic power signal frequency is shown as Equation (11).

$$f_a = f_0 \frac{N_0}{\pi} \tan^{-1}\left(\tan\left(\frac{\pi}{N_0}\right) \cdot R_{atio}\right) \tag{11}$$

However, the filtered signals can be affected by the amplitude responses and the frequency response effects. Therefore, the frequency evaluation using Equations (10) and (11) will be subject to these factors. Equations (12) and (13) are phase response equations that can be used to deduce the 90° angle differences. Thus, we can resolve the phase angle differences and find the ideal amplitude ratios.

$$\angle H_{CosWindow}(f) = \pi - \pi \frac{(N_0 - 1)f}{N_0 \cdot f_0} \tag{12}$$

$$\angle H_{SinWindow}(f) = \frac{1}{2}\pi - \pi \frac{(N_0 - 1)f}{N_0 \cdot f_0} \tag{13}$$

To resolve the phase response effects, a DFT filter is used to determine the amplitude ratio of the filtered sine and cosine signals outputted during the first level. This method uses the phase response characters to offset the filtered signal by 90° to turn the signal phase difference into 180°. Thus, the two orthogonal signals will become symmetrical signals with only the positive and negative sign differences. The vectors of the second level DFT-filtered discrete signals are represented as Equations (14) and (15).

$$A = [A_1 \ A_2 \ A_3 \ .... \ ..... A_n]^T \tag{14}$$

$$B = [B_1 \ B_2 \ B_3 \ .... \ ..... B_n]^T \tag{15}$$

When Equation (10) uses Equations (14) and (15) to calculate the amplitude ratio, the amplitude ratio would have a significant deviation in the vicinity of the zero-crossover for the filtered values A and B, and the frequency calculation would produce an erroneous value. To resolve the zero-crossover problem, the frequency domain difference technique is adapted to verify the amplitude ratio because, in addition to the harmonic or inter-harmonic waves, real signals also contain voltage flickers and other noises. Although this frequency assessment method is based on the DFT filtering technique and can prevent harmonic and inter-harmonic wave interferences, the method still cannot prevent voltage flickers and other signal noise interferences. Thus, the interpolation technique is applied to further suppress the interferences and calculate the precise amplitude value.

 doi:10.20944/preprints201804.0337.v1

2.3. Amplitude Interpolation Method

The discrete time sequence representation of a Hanning window is expressed as [8, 9]:

$$W(n) = 0.5 - 0.5\cos\left(\frac{2\pi n}{N}\right), n = 0,1,...N-1 \tag{16}$$

The spectrum of the dot product of $x(.)$ from Equation (1) and the $W(.)$ from Equation (16) yields Equation (17):

$$X(k) = -\frac{1}{2j}\left[Ae^{j\theta}\cdot W(\lambda - k) - Ae^{j\theta}\cdot W(\lambda + k)\right] \tag{17}$$
$$, k = 0,1,\ldots N-1$$

where k is the frequency index of the DFT at the k-th spectral line; λ is the normalized frequency and can be written in two parts, as indicated in Equation (18) where l is the integer part of the frequency and δ is the fraction part of the frequency.

$$\lambda = \frac{f\cdot N}{f_0\cdot N_0} = l + \delta, -0.5 \le \delta < 0.5 \tag{18}$$

Figure 3 shows the interpolation method of the Fourier transform spectrum where k is the largest index value in the X_k amplitude. When N is large enough, the amplitude can be expressed as:

$$V_k = |X_k| = \frac{N\cdot A\cdot\sin(\pi\delta)}{2\pi\delta} \tag{19}$$

δ is the largest frequency deviation for the true amplitude and the transformed amplitude in the spectrum, the value range of δ is between -0.5–0.5, the left and the right maximum amplitudes have the index values of k-1 and k+1, and its amplitude is expressed as:

$$V_{k\pm1} = |X_{k\pm1}| = \frac{N\cdot A\cdot|\sin(\pi\delta)|}{2\pi(1-|\delta|)} \tag{20}$$

After the sampling signal is multiplied by the Hanning Window, the relationship between the largest amplitude frequency and the second largest amplitude frequency after the transformation—V_k and $V_{k\pm1}$—has the ratio of α which is expressed as:

$$\alpha = \frac{V_{k\pm1}}{V_k} = \frac{1+|\delta|}{2-|\delta|} \tag{21}$$

Through the Hanning Window relationship, the deviation ratio δ is expressed as:

$$\delta = \frac{2\delta - 1}{1+\delta} \tag{22}$$

The amplitude correction value is thus expressed as:

$$V = \frac{2\pi|\delta|(1-\delta^2)}{N\sin(\pi\delta)}V_k \tag{23}$$

Preprints (www.preprints.org) | NOT PEER-REVIEWED | Posted: 26 April 2018 doi:10.20944/preprints201804.0337.v1

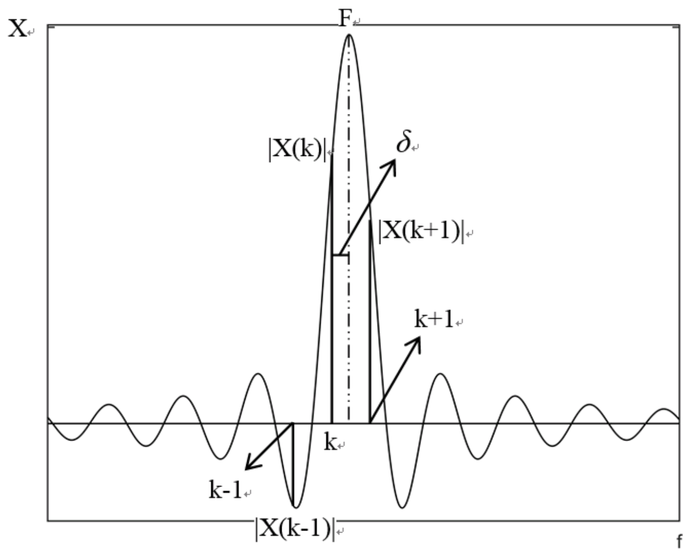

Figure 3. Interpolation algorithm diagram.

Finally, after the amplitude ratio has been incorporated into the frequency domain interpolation using Equations (14) and (15), Equation (23) is used to calculate the corrected orthogonal filter amplitude, and then incorporate the amplitude value into Equation (11) to accurately evaluate the power system frequency.

3. Results

To verify the performance of the two-level DFT and frequency domain interpolation hybrid method proposed in this paper, we performed numerical simulations based on the various voltage signals encountered by the actual power system in a MATLAB simulation environment. They include harmonics, inter-harmonics, flickers, noises, and frequency offsets.

We used four frequency evaluation methods to compare all of the test results: the zero-crossing interpolation waveform reconstruction method (ZCIWR) [5], the frequency-domain interpolated (FDI) [8], the frequency-domain interpolated waveform reconstruction method (FDIWR) [9], and the method proposed in this paper. The objective of the comparisons is to understand the frequency deviations of the frequency estimation methods. The frequency absolute value proposed in [4, 26] is used to calculate the relative error as described in Equation (24).

$$\text{Relative Error}(\%) = \frac{|\text{Actual Value} - \text{Estimated Value}|}{\text{Actual Value}} \times 100\% \tag{24}$$

The IEC 61000-4-7 standard has proposed the 5 Hz frequency resolution recommended value based on the DFT technique. That is, the analysis information with the time length of 0.2 s is applied for harmonic and inter-harmonic analyses. The sampling frequency is 3000 Hz, and the experimental data window length of N is set to 0.2 s. For the ZCIWR method, the frequency can only be calculated near the vicinity of the zero-crossover. To verify the performance frequency evaluation performance, the steady-state data window sliding coefficient was obtained as one cycle, and one frequency calculation was conducted for each cycle. To obtain an accurate and precise conclusion, each simulated measurement was performed 500 times and the average value is used.

3.1. Asynchronous Sampling Basic Frequency Evaluation

The IEC 61000-4-30 standard specifies the accuracy tolerance for measurements made by PQ analysis instruments. The basic frequency offset tolerance range for a power system with a rated frequency of 60 Hz is between 51 Hz and 69 Hz. To test whether the frequency evaluation method can effectively calculate the basic frequency, the simulated wave is represented using Equation (25), where f_a varies between 51 Hz and 69 Hz, and the with 1 Hz offset.

$$x(t) = \cos(2\pi f_a t) \tag{25}$$

Preprints (www.preprints.org) | NOT PEER-REVIEWED | Posted: 26 April 2018 doi:10.20944/preprints201804.0337.v1

Table 1 shows the results according to different frequencies under the various frequency evaluation methods. As anticipated, the proposed method is not affected by the a-th frequency offsets. Table 1 indicated that the deviations derived from the calculation method proposed by this paper are lower than 1e-14.

Table 1. Average relative frequency deviations for different basic frequency offsets.

Frequency Deviation(Hz)	Frequency Evaluation deviation (%)			
	ZCIWR	FDI	FDIWR	Proposed method
51	9.174e-07	3.187e-04	1.087e-10	0
52	4.120e-07	5.431e-05	1.952e-11	9.455e-15
53	2.192e-07	4.192e-04	3.884e-08	8.097e-15
54	1.721e-06	3.191e-04	9.737e-12	1.315e-14
55	1.860e-06	0	1.991e-10	7.027e-15
56	1.649e-06	1.747e-04	4.488e-10	1.268e-14
57	1.934e-06	3.767e-04	1.166e-08	1.246e-14
58	1.784e-06	1.270e-04	6.679e-07	3.381e-15
59	2.671e-06	1.480e-04	2.492e-08	1.204e-14
60	9.852e-13	1.184e-14	0	0
61	1.987e-06	8.175e-05	4.386e-08	1.1648-14
62	1.530e-06	1.784e-04	9.756e-09	1.1460-14
63	2.278e-06	2.697e-04	1.982e-08	0
64	2.987e-06	6.740e-05	4.351e-09	0
65	4.387e-06	0	1.126e-10	0
66	4.756e-06	1.349e-04	2.862e-10	0
67	3.702e-06	1.203e-04	1.599e-09	0
68	3.198e-06	1.211e-04	1.607e-10	0
69	4.031e-06	1.233e-04	4.218e-07	0

3.2. Basic Frequency Evaluation Under Harmonic and Inter-harmonic Environments

In this paper, we referenced the IEC 61000-4-30 standard to propose the harmonic and inter-harmonic verification perimeters. The simulated waveform is represented using Equation (26) where f_a ranged from 51 Hz to 69 Hz and the offsets were made in 1 Hz increments.

$$\begin{aligned} x(t) = {} & \cos(2\pi f_a t) + 0.1\cos(3\times 2\pi f_a t) + 0.05\cos(5\times \pi f_a t) + 0.1\cos(7\times 2\pi f_a t + pi) + 0.05\cos(13\times 2\pi f_a t) \\ & + 0.05\cos(25\times 2\pi f_a t) + 0.05\cos(29\times 2\pi f_a t) + 0.01\cos(3.5\times 2\pi f_a t) + 0.01\cos(7.5\times 2\pi f_a t); \end{aligned} \tag{26}$$

Table 2 indicates that all four techniques are affected by the harmonics and inter-harmonics in the harmonic and inter-harmonic environments. However, the average deviations derived from the frequency evaluation algorithm adopted by this paper under a variety of frequency offsets were all better than those of other methods.

Table 2. Average relative frequency deviation under harmonic and inter-harmonic environment.

Frequency Deviation(Hz)	Frequency Evaluation deviation (%)			
	ZCIWR	FDI	FDIWR	Proposed method
51	9.844e-07	3.781e-04	1.033e-04	3.602e-07

52	3.745e-07	4.233e-05	1.361e-05	4.119e-07
53	2.299e-07	4.126e-04	0.002	6.459e-07
54	1.601e-06	3.411e-04	4.764e-05	3.482e-07
55	1.513e-06	2.122e-06	1.565e-05	1.268e-08
56	1.414e-06	2.246e-04	2.939e-05	1.731e-07
57	1.964e-06	3.731e-04	3.879e-05	3.518e-07
58	1.894e-06	8.510e-05	4.630e-05	5.698e-08
59	2.760e-06	1.372e-04	4.218e-05	3.070e-08
60	9.971e-13	1.184e-14	0	0
61	2.025e-06	8.500e-05	4.233-05	4.798-09
62	1.504e-06	1.762e-04	3.616e-04	8.195e-08
63	2.169e-06	2.601e-04	7.604e-04	8.980e-08
64	2.906e-06	7.771e-05	3.063e-04	1.6156e-08
65	4.542e-06	5.025e-07	7.562e-07	1.372e-09
66	5.133e-06	1.456e-04	7.672e-06	1.004e-08
67	3.765e-06	8.755e-05	0.001	8.496e-08
68	3.364e-06	9.517e-05	0.004	3.193e-08
69	3.843e-06	1.318e-04	0.005	7.024e-08

3.3. Basic Frequency Evaluation Under Flickering Environments

In addition to the harmonic and inter-harmonic frequencies, power system voltages usually also contain flicker frequencies. According to [27], human eyes are most sensitive to a flicker frequency of approximately 8.8 Hz. Thus, we added two flicker components of 5 Hz and 8.8 Hz to Equation (26), with amplitudes of 0.05% and 0.1%, respectively.

Table 3 shows the frequency evaluation deviations of the four methods under the harmonic, inter-harmonic, and flicker interference environments. The relative deviation obtained using the method proposed by this paper was approximately 1e-4%, and was approximately 1e-1% using other methods. Thus, the method proposed by this paper has better performance under the harmonic, inter-harmonic, and flicker interference environments.

Table 3. Average relative frequency deviation under flicker environments.

Frequency Deviation(Hz)	Frequency Evaluation deviation (%)			
	ZCIWR	FDI	FDIWR	Proposed method
51	0.050	0.057	0.348	0.009
52	0.048	0.033	0.277	0.005
53	0.045	0.042	0.16	0.002
54	0.040	0.152	0.018	0.002
55	0.035	0.117	0.188	0.002
56	0.029	0.101	0.047	0.001
57	0.024	0.040	0.084	0.001
58	0.019	0.045	0.191	0.001
59	0.015	0.141	0.227	0.001
60	0.013	0.179	0.179	0.003

Preprints (www.preprints.org) | NOT PEER-REVIEWED | Posted: 26 April 2018 doi:10.20944/preprints201804.0337.v1

61	0.014	0.121	0.251	0.009
62	0.017	0.042	0.272	0.010
63	0.020	0.044	0.246	0.011
64	0.024	0.097	0.283	0.006
65	0.028	0.209	0.270	0.008
66	0.031	0.125	0.219	0.010
67	0.034	0.041	0.140	0.011
68	0.036	0.030	0.238	0.005
69	0.050	0.057	0.348	0.009

3.4. Basic Frequency Evaluation Under Noise Environments

To test whether the frequency estimation algorithm can effectively calculate the basic frequency under a noise interference environment, a 60 dB of noise is added to the simulated waveform discussed in 3.3.

Table 4 shows the maximum relevant deviation from simulating all of the frequency estimation methods 500 times in mixed environments. The table indicates that when using the ZCIWR, FDI, FDIWR, and the method proposed by this paper in mixed interference environments with a steady-state evaluation frequency of between 51–69 Hz; the maximum average relative deviations were 5e-02%, 2e-01%, 3e-01%, and 1e-02%, respectively. The results indicate that all four algorithms had good responses in the 60 dB environment.

Table 4. Maximum relative frequency deviation in a mixed environment.

Frequency Deviation(Hz)	Frequency Evaluation deviation (%)			
	ZCIWR	FDI	FDIWR	Proposed method
51	0.050	0.058	0.347	0.009
52	0.048	0.033	0.278	0.004
53	0.045	0.042	0.160	0.003
54	0.040	0.152	0.019	0.002
55	0.035	0.116	0.181	0.001
56	0.029	0.102	0.047	0.001
57	0.024	0.040	0.083	0.001
58	0.019	0.045	0.191	0.001
59	0.015	0.141	0.227	0.001
60	0.013	0.178	0.175	0.003
61	0.014	0.121	0.251	0.009
62	0.017	0.042	0.272	0.010
63	0.020	0.044	0.246	0.012
64	0.024	0.096	0.282	0.006
65	0.028	0.208	0.269	0.008
66	0.031	0.125	0.219	0.010
67	0.034	0.041	0.140	0.011
68	0.036	0.030	0.238	0.005
69	0.037	0.111	0.166	0.008

4. Conclusion

In this paper, we adopted the classic spectrum analysis algorithm used by the majority of scholars—DFT—as the basis for frequency evaluation for the PQ analysis. A two-level DFT and frequency domain interpolation hybrid technique is used for basic frequency evaluation. This method used the DFT filter as the basis for the frequency calculation. This approach can reduce the harmonic and inter-harmonic interferences. The orthogonal characteristics and the frequency domain interpolation method were then used to further suppress the flicker components. The experimental results indicated that when the signals sampled using the method proposed by this paper contained harmonic, inter-harmonic, and flicker components, the method can obtain high-precision basic frequency that can be used to facilitate subsequent PQ spectrum analyses.

Acknowledgments: This research is supported by the Project of the Ministry of Science and Technology, Taiwan, under grant numbers MOST 104-2221-E-027-060-MY2 and MOST 106-3113-E-006-010.

References

1. Luo, Y.; Kaicheng, L.; Li, Y.; Cai, D.; Zhao, C.; Meng, Q. Three layer bayesian network for classification of complex power quality disturbances. *IEEE Transactions on Industrial Informatics* **2017**, 1-1
2. Camarena-Martinez, D.; Valtierra-Rodriguez, M.; Perez-Ramirez, C.A.; Amezquita-Sanchez, J.P.; Romero-Troncoso, R.d.J.; Garcia-Perez, A. Novel downsampling empirical mode decomposition approach for power quality analysis. *IEEE Transactions on Industrial Electronics* **2016**, *63*, 2369-2378.
3. Singh, U.; Singh, S.N. Optimal feature selection via nsga-ii for power quality disturbances classification. *IEEE Transactions on Industrial Informatics* **2017**, 1-1.
4. Cheng, I.C. Design of measurement system based on signal reconstruction for analysis and protection of distributed generations. *IEEE Transactions on Industrial Electronics* **2013**, *60*, 1652-1658.
5. Zhou, F.; Huang, Z.; Zhao, C.; Wei, X.; Chen, D. Time-domain quasi-synchronous sampling algorithm for harmonic analysis based on newton's interpolation. *IEEE Transactions on Instrumentation and Measurement* **2011**, *60*, 2804-2812.
6. Djurić, M.B.; Djurišić, Ž.R. Frequency measurement of distorted signals using fourier and zero crossing techniques. *Electric Power Systems Research* **2008**, *78*, 1407-1415.
7. Chen, Y.-C.; Chien, T.-H. *A simple approach for power signal frequency determination on virtual instrument platform*. 2015; Vol. 9, p 65-71.
8. Agrez, D. Weighted multipoint interpolated dft to improve amplitude estimation of multifrequency signal. *IEEE Transactions on Instrumentation and Measurement* **2002**, *51*, 287-292.
9. Chang, G.; Chen, C.I.; Liu, Y.J.; Wu, M.C. *Measuring power system harmonics and interharmonics by an improved fast fourier transform-based algorithm*. 2008; Vol. 2, p 193-201.
10. Nam, S.-R.; Kang, S.-H.; Kang, S.-H. Real-time estimation of power system frequency using a three-level discrete fourier transform method. *Energies* **2015**, *8*, 79.
11. Jun-Zhe, Y.; Chih-Wen, L. A precise calculation of power system frequency and phasor. *IEEE Transactions on Power Delivery* **2000**, *15*, 494-499.
12. Belega, D.; Petri, D. Accuracy analysis of the multicycle synchrophasor estimator provided by the interpolated dft algorithm. *IEEE Transactions on Instrumentation and Measurement* **2013**, *62*, 942-953.
13. Macii, D.; Petri, D.; Zorat, A. Accuracy analysis and enhancement of dft-based synchrophasor estimators in off-nominal conditions. *IEEE Transactions on Instrumentation and Measurement* **2012**, *61*, 2653-2664.
14. Reza, S.; Ciobotaru, M.; Agelidis, V.G. Accurate estimation of single-phase grid voltage fundamental amplitude and frequency by using a frequency adaptive linear kalman filter. *IEEE Journal of Emerging and Selected Topics in Power Electronics* **2016**, *4*, 1226-1235.
15. Talebi, S.P.; Kanna, S.; Mandic, D.P. A distributed quaternion kalman filter with applications to smart grid and target tracking. *IEEE Transactions on Signal and Information Processing over Networks* **2016**, *2*, 477-488.
16. Golestan, S.; Guerrero, J.M.; Vasquez, J.C. A pll-based controller for three-phase grid-connected power converters. *IEEE Transactions on Power Electronics* **2018**, *33*, 911-916.
17. Golestan, S.; Guerrero, J.M.; Vasquez, J.C. A nonadaptive window-based pll for single-phase applications. *IEEE Transactions on Power Electronics* **2018**, *33*, 24-31.
18. Reza, M.S.; Ciobotaru, M.; Agelidis, V.G. Power system frequency estimation by using a newton-type technique for smart meters. *IEEE Transactions on Instrumentation and Measurement* **2015**, *64*, 615-624.

19. Nanda, S.; Dash, P.K. A gauss–newton adaline for dynamic phasor estimation of power signals and its fpga implementation. *IEEE Transactions on Instrumentation and Measurement* **2018**, *67*, 45-56.
20. Xia, Y.; Blazic, Z.; Mandic, D.P. Complex-valued least squares frequency estimation for unbalanced power systems. *IEEE Transactions on Instrumentation and Measurement* **2015**, *64*, 638-648.
21. Ž, Z.; Krstajić, B.; Popović, T. Improved frequency estimation in unbalanced three-phase power system using coupled orthogonal constant modulus algorithm. *IEEE Transactions on Power Delivery* **2017**, *32*, 1809-1816.
22. Lobos, T.; Rezmer, J. Real-time determination of power system frequency. *IEEE Trans. Instrum. Meas.* **1997**, *46*, 877–881.
23. Khodaparast, J.; Khederzadeh, M. Dynamic synchrophasor estimation by taylor–prony method in harmonic and non-harmonic conditions. *IET Generation, Transmission & Distribution* **2017**, *11*, 4406-4413.
24. Fu, L.; Zhang, J.; Xiong, S.; He, Z.; Mai, R. A modified dynamic synchrophasor estimation algorithm considering frequency deviation. *IEEE Transactions on Smart Grid* **2017**, *8*, 640-650.
25. Coury, D.V.; Delbem, A.C.B.; Carvalho, J.R.d.; Oleskovicz, M.; Simoes, E.V.; Barbosa, D.; Silva, T.V.d. Frequency estimation using a genetic algorithm with regularization implemented in fpgas. *IEEE Transactions on Smart Grid* **2012**, *3*, 1353-1361.
26. Gupta, P.; Bhatia, R.S.; Jain, D.K. Average absolute frequency deviation value based active islanding detection technique. *IEEE Transactions on Smart Grid* **2015**, *6*, 26-35.
27. Bai, F.; Wang, X.; Liu, Y.; Liu, X.; Xiang, Y.; Liu, Y. Measurement-based frequency dynamic response estimation using geometric template matching and recurrent artificial neural network. *CSEE Journal of Power and Energy Systems* **2016**, *2*, 10-18.